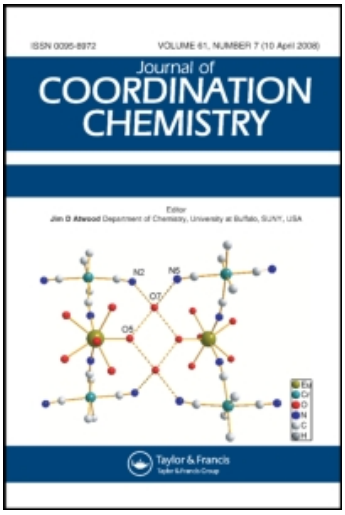

Journal of Coordination Chemistry
Publication details, including instructions for authors and subscription information:
http://www.informaworld.com/smpp/title~content=t713455674

X-ray structure of $[Re(NO)_{2.09}Br_{1.91}(PPh_3)_2]$ and DFT studies of $[Re(NO)_2Br_2(PPh_3)_2]$

B. Machura[a]; R. Kruszynski[b]
[a] Department of Inorganic and Radiation Chemistry, Institute of Chemistry, University of Silesia, 40-006 Katowice, Poland [b] Department of X-Ray Crystallography and Crystal Chemistry, Institute of General and Ecological Chemistry, Łódź University of Technology, 90-924 Łódź, Poland

To cite this Article Machura, B. and Kruszynski, R.(2006) 'X-ray structure of $[Re(NO)_{2.09}Br_{1.91}(PPh_3)_2]$ and DFT studies of $[Re(NO)_2Br_2(PPh_3)_2]$', Journal of Coordination Chemistry, 59: 4, 445 — 456
To link to this Article: DOI: 10.1080/00958970500490897
URL: http://dx.doi.org/10.1080/00958970500490897

Journal of Coordination Chemistry
Vol. 59, No. 4, March 2006, 445–456

Taylor & Francis
Taylor & Francis Group

X-ray structure of $[Re(NO)_{2.09}Br_{1.91}(PPh_3)_2]$ and DFT studies of $[Re(NO)_2Br_2(PPh_3)_2]$

B. MACHURA*† and R. KRUSZYNSKI‡

†Department of Inorganic and Radiation Chemistry, Institute of Chemistry, University of Silesia, 9th Szkolna Street, 40-006 Katowice, Poland
‡Department of X-Ray Crystallography and Crystal Chemistry, Institute of General and Ecological Chemistry, Łódź University of Technology, 116 Żeromski Street, 90–924 Łódź, Poland

(*Received in final form 27 September 2005*)

The crystal and molecular structure of $[Re(NO)_{2.09}Br_{1.91}(PPh_3)_2]$ and DFT studies of $[Re(NO)_2Br_2(PPh_3)_2]$ are reported. The linearly bonded nitrosyl ligands adopt *cis* geometry, and two bulky triphenylphosphine molecules occupy axial positions of a distorted octahedral coordination sphere. The *cis*-nitrosyl grouping with respect to PPh_3 molecules (π-acid ligands) is the result of the electronic influence of the multiply bonded ligand, which forces the metal nonbonding d electrons to lie in the plane perpendicular to the M–NO bond axis.

Keywords: Rhenium; Phosphine; Nitrosyl; X-ray structure; DFT calculations

1. Introduction

For many years attention has been focussed on the synthesis and study of transition metal nitrosyl complexes. These have been at the centre of interest of scientists engaged both in basic research and trying to employ these complexes in catalysis, production of organonitrogen compounds and pollutant control (reduction of NO in exhaust fumes). The recent discovery of the key role of nitric oxide in human cardiovascular and nervous systems, and in immune response to pathogen invasion, has resulted in added interest in nitrosyl complexes [1–16].

One of the most important aspects of t research on nitrosyl complexes is the determination of the bonding nature of NO to the metal centre. The NO molecule can bind to a metal centre via N or O atoms to give nitrosyl (M–NO) or isonitrosyl (M–ON) species, respectively. In practice, the bonding of NO involves attachment of the N atom to the metal centre, and M–N–O angles may be essentially linear or bent, up to ca 120°.

Historically, the bonding of the M–NO unit has been described by assigning formal oxidation states to the metal centre and the nitrosyl ligand. In such an assignment,

*Corresponding author. Email: bmachura@poczta.onet.pl

Journal of Coordination Chemistry
ISSN 0095-8972 print: ISSN 1029-0389 online © 2006 Taylor & Francis
DOI: 10.1080/00958970500490897

a linear M–NO unit is deemed to possess a bound NO^+ ligand, and conversely, a bent M–NO core is deemed to possess a bound NO^- ligand. In the Enemark-Feltham formalism nitrosyl-containing species are described as $\{MNO\}^n$ (regardless of co-ligands), where n stands for the number of electrons associated with the metal d and π^*(NO) orbitals. The extension of Walsh's concepts to the $\{MNO\}^n$ group can be used to predict the bond angle of the $\{MNO\}^n$ unit on the basis of n. In a molecular orbital approach, the bonding of NO to a metal is considered to be made up of two components. The first donation of electron density from a σ-type orbital of NO onto the metal, and the second involves back donation from the metal d orbitals to π^* orbitals of NO [1–16].

Previously, we investigated the reactivity of $[ReOX_3L_2]$ compounds (X = Cl and Br, L = PPh_3 and $AsPh_3$) towards gaseous nitric oxide and various products were isolated, depending on reaction conditions, including $[ReX_3(NO)(OPPh_3)_2]$, $[ReX_2(NO)_2(PPh_3)_2]$, $[ReBr_3(NO)(MeCN)(PPh_3)]$, $[ReCl_3(NO)(PPh_3)(OPPh_3)]$, $[ReCl_4(PPh_3)_2]$, $[ReX_3(NO)(OAsPh_3)_2]$, $[ReCl_4(OAsPh_3)_2]$ and $[ReCl_3(NO)(AsPh_3)_2]$ $[ReCl_4(AsPh_3)_2]$ [17–23]. All complexes were characterised spectroscopically. X-Ray structures, however, were determined only for the mononitrosyl compounds. Here, we present the crystal and molecular structure of $[Re(NO)_{2.09}Br_{1.91}(PPh_3)_2]$ and DFT studies of $[Re(NO)_2Br_2(PPh_3)_2]$. Currently, density functional theory (DFT) is commonly used to examine the electronic structure of transition metal complexes. It meets with the requirements of being accurate, easy to use and fast enough to allow the study of relatively large transition metal complexes [24–28]. Additional information concerning binding in the $\{Re(NO)_2\}^7$ unit of $[Re(NO)_2Br_2(PPh_3)_2]$ was obtained by NBO analysis.

2. Experimental

$[Re(NO)_{2.09}Br_{1.91}(PPh_3)_2]$ was prepared according to a literature method [17].

2.1. *Crystal structure*

X-ray intensities were collected on a KM-4-CCD automatic diffractometer equipped with a CCD detector. A 20 second exposure time was used and reflections were collected up to $\theta = 25^\circ$. Unit cell parameters were determined from least-squares refinement of the setting angles of 5463 strongest reflections. Details concerning crystal data and refinement are given in table 1. Lorentz, polarization and numerical absorption corrections [29] were applied. The structure was solved by the Patterson method and subsequently completed by difference Fourier cycles. All non-hydrogen atoms were refined anisotropically using full-matrix, least-squares techniques. Hydrogen atoms bonded to the aromatic atoms were treated as riding on their parent carbon atoms and assigned isotropic temperature factors equal to 1.2 times the value of equivalent isotropic temperature factor of the parent atom. SHELXS97 [30], SHELXL97 [31] and SHELXTL [32] programs were used for all calculations. Atomic scattering factors were those incorporated in the computer programs.

Table 1. Crystal data and structure refinement details for $[Re(NO)_{2.09}Br_{1.91}(PPh_3)_2]$.

Empirical formula	$C_{36}H_{30}Br_{1.91}N_{2.09}O_{2.09}P_2Re$
Formula weight	926.21
Temperature (k)	291(2)
Wavelength (Å)	0.71073
Crystal system	Monoclinic
Space group	$C2/c$
Unit cell dimensions (Å, °)	$a = 24.668(3)$ $b = 9.5648(8)$ $\beta = 115.837(9)$ $c = 16.2681(19)$
Volume (Å^3)	3454.7(6)
Z	4
Density (calculated) (Mg m^{-3})	1.781
Absorption coefficient (mm^{-1})	5.857
$F(000)$	1797
Crystal size (mm^3)	$0.22 \times 0.19 \times 0.18$
θ range for data collection (°)	3.27 to 25.11
Index ranges	$-29 \le h \le 29$, $-11 \le k \le 11$, $-19 \le l \le 17$
Reflections collected	17847
Independent reflections	3090 ($R_{int} = 0.0443$)
Completeness to 2θ	46.9%
Data/restraints/parameters	3090/0/220
Goodness-of-fit on F^2	1.190
Final R indices [$I > 2\sigma(I)$]	$R_1 = 0.0270$ $wR_2 = 0.0517$
R indices (all data)	$R_1 = 0.0306$ $wR_2 = 0.0528$
Largest diff. peak and hole (e Å^{-3})	0.571 and −0.788

2.2. *Computational details*

The Gaussian03 program [33] was used in the calculations. Geometry optimisation of $[Re(NO)_2Br_2(PPh_3)_2]$ was carried out with the DFT method using the B3LYP function [34, 35]. The calculations were performed using the ECP basis set for the rhenium atom, the standard 6-31 g* basis for bromine, oxygen, phosphorous, nitrogen, carbon and the 6-31 G basis for hydrogen atoms. Xe core electrons of Re were replaced by an effective core potential and the DZ quality Hay and Wadt Los Alamos ECP basis set (LANL2DZ) [36] was used for valence electrons. Additional d with exponent $\alpha = 0.3811$ and f with exponent $\alpha = 2.033$ functions were added to the rhenium atom. Natural bond orbital (NBO) calculations were performed with the NBO code [37] included in Gaussian03.

3. Results and discussion

3.1. *Structure*

The complex isolated in the reaction of $[ReOBr_3(PPh_3)_2]$ with gaseous nitric oxide [17] was formulated as $[Re(NO)_2Br_2(PPh_3)_2]$. The X-ray studies, however, show nitrosyl/bromine compositional disorder in the structure of the dinitrosyl complex. As a result of the disorder the formula is $[Re(NO)_{2.09}Br_{1.91}(PPh_3)_2]$. The amount of nitrosyl substituent is slightly larger than 2 and it can be supposed that this difference originates

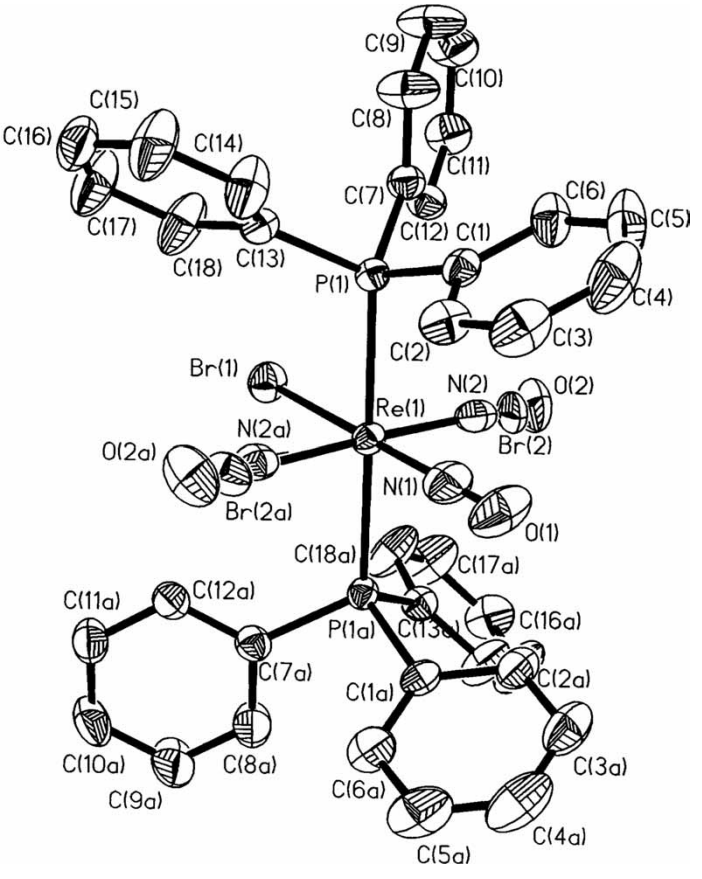

Figure 1. Thermal ellipsoid plot of $[Re(NO)_{2.09}Br_{1.91}(PPh_3)_2]$ showing the atom numbering scheme (50% probability ellipsoids).

from experimental errors. To verify this hypothesis X-ray data were refined with a fixed $[Re(NO)_2Br_2(PPh_3)_2]$ formula. Displacement ellipsoids of the disordered bromine ions were abnormally large, and displacement ellipsoids of disordered NO groups unusually small, and thus it is concluded that $[Re(NO)_{2.09}Br_{1.91}(PPh_3)_2]$ is the correct formula for the crystals investigated.

$[Re(NO)_{2.09}Br_{1.91}(PPh_3)_2]$ complex crystallises in the monoclinic space group $C2/c$ with Re and ordered Br and NO substituents lying on a crystallographic two-fold rotation axis. Refinement of the structure in non-centrosymmetric space groups $C2$ and Cc did not change the disordered atom composition and the Flack parameter was equal to 0.5 in both cases; thus space group $C2/c$ was selected as the correct one. The complex is isomorphous with $[ReX_3(NO)(PPh_3)_2]$ (X = Cl and Br) [22, 23], $[ReOCl_3(PPh_3)_2]$ [38] and several similar ruthenium nitrosyl compounds [39, 40]. The packing of the two bulky triphenylphosphine ligands, which lie *trans* to each other, seems to govern the solid state structure. The atom numbering scheme of the disordered $[Re(NO)_{2.09}Br_{1.91}(PPh_3)_2]$ complex is shown in figure 1. The *trans* arrangement of the two bulky triphenylphosphine molecules causes the *cis* location of the nitrosyl groups with respect to PPh_3 (π-acid ligands). This is due to the electronic influence of the

Table 2. Bond lengths (Å) and angles (°) for $[Re(NO)_{2.09}Br_{1.91}(PPh_3)_2]$ and optimised bond lengths (Å) and angles (°) for $[Re(NO)_2.Br_2(PPh_3)_2]$.

Bond lengths			Bond angles		
	Experimental	Optimized		Experimental	Optimized
Re(1)–N(1)	1.866(5)	1.814	N(1)–Re(1)–N(2)	89.9(4)	97.9
Re(1)–N(2)	1.966(14)	1.821	N(1)–Re(1)–P(1)	90.45(2)	92.7
Re(1)–P(1)	2.5092(9)	2.568	N(2)–Re(1)–P(1)	92.5(4)	92.7
Re(1)–P(1)	2.5092(9)	2.568	N(1)–Re(1)–Br(2)	86.36(7)	83.0
Re(1)–Br(1)	2.5917(6)	2.679	P(1)–Re(1)–Br(2)	92.29(6)	87.4
Re(1)–Br(2)	2.539(2)	2.662	N(1)–Re(1)–Br(1)	180.0	174.3
N(1)–O(1)	1.166(6)	1.184	N(2)–Re(1)–Br(1)	90.1(4)	87.7
N(2)–O(2)	1.09(2)	1.183	P(1)–Re(1)–Br(1)	89.55(2)	87.0
			Br(2)–Re(1)–Br(1)	93.64(7)	91.4
			P(1)–Re(1)–Br(2)#1	87.77(6)	87.4
			N(2)–Re(1)–P(1)#1	87.5(4)	92.5
			N(2)–Re(1)–Br(2)#1	176.2(4)	179.1
			P(1)#1–Re(1)–P(1)	179.09(4)	172.0
			P(1)#1–Re(1)–Br(1)	89.55(2)	87.1
			O(1)–N(1)–Re(1)	180.0	179.1
			O(2)–N(2)–Re(1)	178.3(16)	175.3

Equivalent position #1 at $-x, y, -z+1/2$.

multiply bonded ligand, which forces the metal nonbonding d electrons to lie in the plane perpendicular to the M–NO bond axis. The linear M–NO groups adopt a *cis* geometry. A *trans* arrangement of nitrosyl groups was confirmed only for the $[Re(NO)_2(pc)]^-$ anion [41]. In all the other structurally characterised mononuclear dinitrosyl rhenium complexes NO ligands adopt a bent structure [42–45]. Two intramolecular hydrogen bonds [46, 47] linking N(12)–H(12)···N(2) (D···A distance 3.330(14) Å and D–H···A angle 135.7°) and C(18)–H(18)···Br(1) (D···A distance 3.718(5) Å and D–H···A angle 148.1°) provide additional stabilisation of the structure. Except for these, no other short contacts were evident. Significant bond lengths and angles for $[Re(NO)_{2.09}Br_{1.91}(PPh_3)_2]$ are reported in table 2. The Re–NO and N–O bond lengths compare well with values found for the other $\{Re(NO)_2\}^7$ complexes [42]. Significant differences in Re–NO and N–O for the two nitrosyl groups of $[Re(NO)_{2.09}Br_{1.91}(PPh_3)_2]$ result from nitrosyl/bromine compositional disorder. Similarly, due to the disorder differences are observed for Re–Br(1) and Re–Br(2) bonds.

3.2. *Optimized geometry*

The geometry of $[Re(NO)_2Br_2(PPh_3)_2]$ was optimised in a doublet state by the DFT method with the B3LYP function. The doublet state agrees well with the experimental value of the effective magnetic moment (1.76 BM) for $[Re(NO)_2Br_2(PPh_3)_2]$. Optimized geometrical parameters for the complex are given in table 2. In general, predicted bond lengths and angles are in good agreement with values based upon the X-ray crystal structure. It is noted, however, that optimised Re–N distances for the two nitrosyl groups differ only by ~0.01 Å, while in the crystal structure this difference is about 0.1 Å. The differences result from nitrosyl/bromine disorder.

3.3. *Charge distribution*

Table 3 lists atomic charges from a Natural Population Analysis (NPA) for $[Re(NO)_2Br_2(PPh_3)_2]$. In the Enemark-Feltham notation the metal-nitrosyl unit of the complex under investigation should be $\{Re(NO)_2\}^7$. The charges on the nitrogen atoms of the nitrosyl groups are positive, whereas the oxygen atoms are negatively charged. Total charges on NO groups of $[Re(NO)_2Br_2(PPh_3)_2]$ are equal to -0.09 and -0.095, and they are far from the expected value $+1$ for a linearly bonded nitrosyl ligand. Consequently, the calculated charge on the rhenium atom of $[Re(NO)_2Br_2(PPh_3)_2]$ is larger than the formal charge 0. In comparison with previously examined $\{Re(NO)\}^5$ mononitrosyls [48–50], the nitrosyl groups of $[Re(NO)_2Br_2(PPh_3)_2]$ are more negatively polarized. This indicates the stronger electron acceptor ability of NO ligands in the dinitrosyl complex.

3.4. *Electronic structure*

The energies and characters of several highest occupied and lowest unoccupied molecular orbitals of $[Re(NO)_2Br_2(PPh_3)_2]$ are presented in tables 4 and 5, respectively. For the molecular orbitals of more complicated character, the percent participations of atomic orbitals are given in round brackets. Figure 2 illustrates selected HOMO and LUMO orbitals of the dinitrosyl complex with α spin. The Br(1)–Re–N(1) linkage was defined as the z axis; x and y axes correspond to Br–Re–N directions.

As mentioned above, the Re–NO bond consists of two components, donation of electron density from a σ-type orbital on NO onto the metal orbital and donation of electron density from the occupied metal d-orbitals into the π^* antibonding orbitals of NO. The occupied d_{xy}, d_{yz} and d_{xz} rhenium orbitals participate in back-donation. The $d_{xy}/d_{yz}/d_{xz}$ and π^*_{NO} orbitals are distributed among several MOs of $[Re(NO)_2Br_2(PPh_3)_2]$ to give contributions to some HOMO (H-21, H-18, H-17, H-5, H-4 and H-2 with α spin and H-18, H-17, H-16, H-9, H-4, H-2 and H-1 with β spin) and LUMO orbitals (L, L + 1, L + 3 with α spin and L + 1, L + 3, L + 6, L + 7, L + 8, L + 12 with β spin). The largest contribution of the bonding $\pi_{Re–NO}$ interaction is visible in H-21, H-18, H-17 with α spin and H-18, H-17, H-16 with β spin. The orbitals H-5, H-4 and H-2 with α spin and H-9, H-4, H-2 and H-1 with β spin are mainly localised on the bromine or phenyl ring orbitals. L, L + 1, L + 3 with α spin and L + 1, L + 3 and L + 8 with β spin are mainly of the $\pi^*_{Re–NO}$ character. Bonding $\pi_{Re–NO}$ orbitals with α and β

Table 3. Atomic charges from the Natural Population Analysis (NPA) of $[Re(NO)_2Br_2(PPh_3)_2]$.

Atom	Atomic charge
Re(1)	0.139
Br(1)	−0.443
Br(2)	−0.450
P(1)	1.400
P(2)	1.400
N(1)	0.143
O(1)	−0.233
N(2)	0.145
O(2)	−0.240

Table 4. The energy and character of selected occupied molecular orbitals with α and β spin for $[Re(NO)_2Br_2(PPh_3)_2]$. The percent participation of the atomic orbitals is given in round brackets.

	α MO		β MO	
	E (eV)	Character	E (eV)	Character
HOMO–21	−8.162	$d_{xy}(38.9) + \pi^*_{NO}(49.1)$; $\pi_{Br}(10.5)$	−8.493	n(P)(35.7), $\sigma_{Ph}(45.4)$, $\pi_{Br}(7.7)$
HOMO–20	−7.942	$\sigma/\pi_{Br}(60.0)$; $d_{x^2-y^2}(19.0)$; π^*_{NO} (14.4)	−7.993	$\sigma/\pi_{Br}(50.4)$; $d_{x^2-y^2}(30.1)$; $\pi^*_{NO}(13.5)$
HOMO–19	−7.882	$\sigma/\pi_{Br}(62.5)$; $d_{x^2-y^2}(18.0)$; π^*_{NO} (11.6)	−7.813	$\sigma/\pi_{Br}(61.0)$; $d_{x^2-y^2}(20.1)$; $\pi^*_{NO}(16.5)$
HOMO–18	−7.682	$d_{yz}(37.4) + \pi^*_{NO}(19.4)$; $\pi_{Ph}(22.7)$; $\pi_{Br}(19.1)$	−7.712	$d_{yz}(41.7) + \pi^*_{NO}(16.5)$; $\pi_{Br}(18.6)$
HOMO–17	−7.462	$d_{xz}(33.9) + \pi^*_{NO}(18.5)$; $\pi_{Ph}(34.9)$; $\pi_{Br}(10.1)$	−7.611	$d_{xy}(34.2) + \pi^*_{NO}(30.3)$; $\pi_{Br}(30.1)$
HOMO–16	−7.251	π_{Ph}	−7.490	$d_{xz}(39.1) + \pi^*_{NO}(16.1)$; $\pi_{Ph}(32.2)$; $\pi_{Br}(9.0)$
HOMO–15	−7.183	π_{Ph}	−7.247	π_{Ph}
HOMO–14	−7.063	π_{Ph}	−7.196	π_{Ph}
HOMO–13	−7.021	π_{Ph}	−7.064	π_{Ph}
HOMO–12	−7.001	π_{Ph}	−7.020	π_{Ph}
HOMO–11	−6.925	π_{Ph}	−7.004	π_{Ph}
HOMO–10	−6.903	π_{Ph}	−6.925	π_{Ph}
HOMO–9	−6.897	π_{Ph}	−6.906	$\pi_{Ph}(73.1)$; $d_{yz}(17.1) + \pi^*_{NO}(7.2)$
HOMO–8	−6.871	π_{Ph}	−6.897	π_{Ph}
HOMO–7	−6.741	π_{Ph}	−6.866	π_{Ph}
HOMO–6	−6.733	π_{Ph}	−6.741	π_{Ph}
HOMO–5	−6.571	$\pi_{Ph}(58.1)$; $d_{xz}(18.5) + \pi^*_{NO}(11.9)$	−6.732	π_{Ph}
HOMO–4	−6.277	$\pi_{Br}(64.5)$, $d_{xy}(6.2) + \pi^*_{NO}(17.5)$	−6.539	$\pi_{Ph}(57.3)$; $d_{yz}(20.9) + \pi^*_{NO}(9.7)$
HOMO–3	−6.191	π_{Br}	−6.171	π_{Br}
HOMO–2	−6.018	$\pi_{Br}(60.7)$, $d_{xz}(10.9) + \pi^*_{NO}(13.8)$; $\pi_{Ph}(14.4)$	−6.059	$\pi_{Br}(61.5)$, $d_{xy}(20.2) + \pi^*_{NO}(12.6)$
HOMO–1	−5.883	$\pi_{Br}(52.1)$; $n_P(19.5)$; $\pi_{Ph}(15.9)$	−6.002	$\pi_{Br}(61.6)$, $d_{xz}(13.6) + \pi^*_{NO}(10.4)$
HOMO	−4.773	π^*_{NO}	−5.892	$\pi_{Br}(54.3)$; $n_P(18.1)$

Table 5. The energy and character of the selected unoccupied molecular orbitals with α and β spin for $Re(NO)_2Br_2(PPh_3)_2]$. The percent participation of the atomic orbitals is given in round brackets.

	α MO		β MO	
	E (eV)	Character	E (eV)	Character
LUMO	−0.061	$\pi^*_{NO}(45.9) - d_{yz}(34.6)$	−1.786	π^*_{NO}
LUMO + 1	−0.050	$\pi^*_{NO}(57.9) - d_{xz}(24.7)$	−1.431	$\pi^*_{NO}(47.5) - d_{yz}(32.7)$
LUMO + 2	−0.048	$d_{z^2}(38.4) - \sigma_P - \sigma_{Br}$; $\pi^*_{NO}(6.1)$	−1.301	$d^2_z(35.8) - \sigma_P - \sigma_{Br}$; $\pi^*_{NO}(3.6)$; $\pi^*_{Ph}(26.2)$
LUMO + 3	−0.035	$\pi^*_{NO}(27.0) - d_{xy}(38.8)$; $\pi^*_{Ph}(21.8)$	−1.097	π^*_{NO} (55.3) − $d_{xz}(17.5)$
LUMO + 4	−0.029	$\pi^*_{Ph}(78.5)$; P(12.5)	−0.811	$\pi^*_{Ph}(78.5)$; P(13.8)
LUMO + 5	−0.026	$\pi^*_{Ph}(86.5)$; P(7.7)	−0.687	$\pi^*_{Ph}(77.4)$; P(16.2)
LUMO + 6	−0.025	$\pi^*_{Ph}(75.0)$; P(18.0)	−0.675	$\pi^*_{Ph}(82.1)$; P(6.9); $\pi^*_{NO}(7.5) - d_{yz}(3.3)$
LUMO + 7	−0.022	$\pi^*_{Ph}(80.0)$; P(11.3)	−0.599	$\pi^*_{Ph}(76.8)$; P(10.8); $\pi^*_{NO}(4.7) - d_{xz}(7.6)$
LUMO + 8	−0.014	$\pi^*_{Ph}(79.1)$; P(9.1); $d_{xz}(9.7)$	−0.409	$\pi^*_{Ph}(47.5)$; $\pi^*_{NO}(15.2) - d_{xy}(23.2)$
LUMO + 9	−0.012	π^*_{Ph}	−0.388	$\pi^*_{Ph}(78.7)$; P(9.3); $d_{xz}(9.2)$
LUMO + 10	−0.010	π^*_{Ph}	−0.323	π^*_{Ph}
LUMO + 11	−0.008	$\pi^*_{Ph}(67.8)$; $d_{z^2}(15.2)$	−0.266	π^*_{Ph}
LUMO + 12	−0.001	π^*_{Ph}	−0.073	$\pi^*_{Ph}(69.9)$; $\pi^*_{NO}(13.5) - d_{xy}(11.9)$
LUMO + 13	0.003	$d_{x^2-y^2}(40.0) - \sigma_P - \sigma_{Br}$; $\pi^*_{Ph}(22.1)$	−0.042	π^*_{Ph}
LUMO + 14	0.003	$\pi^*_{Ph}(75.2)$; $d_{x^2-y^2}(11.8)$	−0.095	π^*_{Ph}
LUMO + 15	0.004	π^*_{Ph}	0.117	π^*_{Ph}

spin are localised mainly on the rhenium d orbitals, whereas the π^*_{Re-NO} orbitals have prevalent NO character. The HOMO with α spin and LUMO with β-spin are localised on the π-antibonding orbitals of the NO groups. The d^2_z rhenium orbital makes contribution into the LUMO + 2 orbitals with α and β spin. Both molecular orbitals have admixture of the π-antibonding orbitals of the NO ligands.

In some of the lowest unoccupied molecular orbitals of π^*_{Ph} character, the contribution of the phosphorous orbitals is visible. In classical concepts empty phosphorous 3*d* orbitals are used in π-back bonding between the metal centre and the phosphine ligand. Now it is generally recognised that the d orbitals are very high in energy and play only a minor role in the π_{M-PR3} bond formation. In π-back bonding between the metal centre and phosphine, the σ^*(P–C) orbitals are involved [51].

3.5. *NBO analysis*

Table 6 presents the occupancies and hybridization of the calculated natural bond orbitals (NBOs) in the $\{Re(NO)_2\}^7$ unit. In accordance with the simple bond orbital picture each bonding NBO orbital can be written in terms of two directed valence hybrids, h_A, h_B, on atoms A and B, with corresponding polarization coefficients c_A, c_B, $\sigma_{AB} = c_A h_A + c_B h_B$. Each valence bonding NBO is paired with a corresponding valence antibonding NBO, $\sigma^*_{AB} = c_B h_A - c_A h_B$, to complete the span of the valence space. As in open-shell systems the density operator separates into distinct components for α and β spin, some differences between NBOs with with α and β spins [52] can be noticed. Table 6 also shows the occupancies and atomic orbital compositions of the lone pair (LP) orbitals detected on N and O atoms of the nitrosyl ligands.

Two natural bond orbitals (one with α spin and one with β spin) were detected for the Re(1)–N(1) bond, four NBOs (two with α spin and two with β spin) for the Re(1)–N(2) bond, three orbitals (one with α-spin and two with β-spin) for the N(1)–O(1) bond and

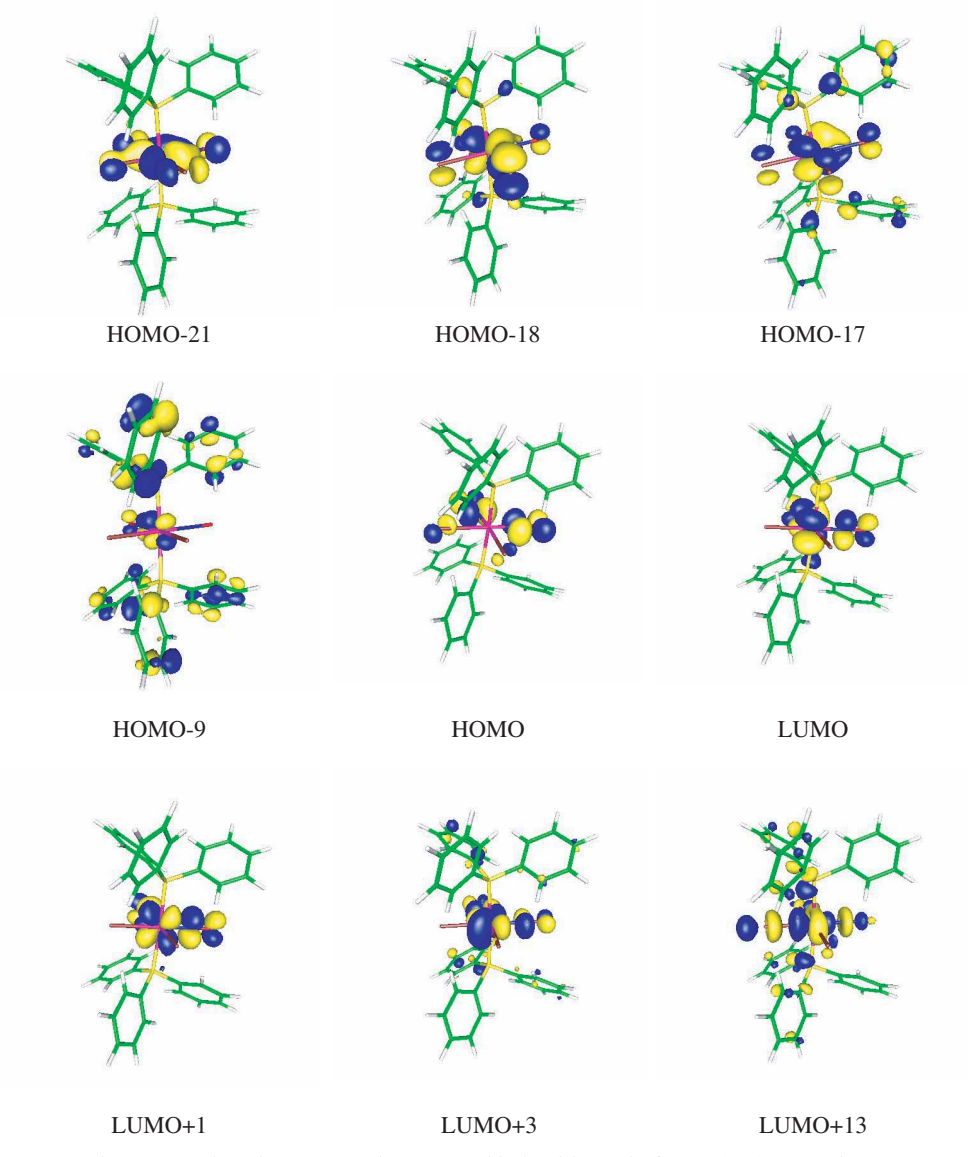

Figure 2. Selected HOMO and LUMO orbitals with α-spin for $[Re(NO)_2Br_2(PPh_3)_2]$.

two NBOs (one with α spin and one with β spin) for the N(2)–O(2) bond. Re(1)–N(1) bond orbitals with α and β spins are mainly polarized towards the metal atom, and the p nitrogen orbitals and d rhenium orbitals take part in Re–N bond formation. The atomic orbital compositions of the Re(1)–N(1) bond orbitals indicate their π character. Undetected $\sigma_{Re(1)–N(1)}$ and $\sigma_{Re(1)–N(2)}$ bond orbitals have predominantly Coulomb-type interaction character between the central ion and the ligand. Three lone pair (LP) NBOs (two with α-spin and one with β-spin) were detected on the N(1) atom, and two LP orbitals (one with α-spin and one with β-spin) on the N(2) atom. The Re(1)–N(1) bond can be considered as being a double bond and the Re(1)–N(2) bond is a triple bond.

Table 6. Occupancies and hybridization of calculated natural bond orbitals (NBOs) in $\{Re(NO)_2\}^7$ for $[Re(NO)_2Br_2(PPh_3)_2]$.

	Occupancy	Hybridization of NBO	Occupancy	Hybridization of NBO
BD		α spin		β-spin
Re(1)–N(1)	0.983(0.260)	$0.779(d)_{Re} + 0.628(p)_N$	0.981(0.287)	$0.828(d)_{Re} + 0.561(p)_N$
N(1)–O(1)	0.998 (0.006)	$0.669(sp^{2.01})_N + 0.743(sp^{2.30})_O$	0.998 (0.008)	$0.668(sp^{1.97})_N + 0.744(sp^{2.25})_O$
			0.996 (0.138)	$0.610(p)_N + 0.793(p)_O$
Re(1)–N(2)	0.987 (0.349)	$0.550(d)_{Re} + 0.835(p)_N$	0.982 (0.284)	$0.825(d)_{Re} + 0.565(p)_N$
	0.984 (0.256)	$0.776(d)_{Re} + 0.631(p)_N$	0.882 (0.311)	$0.857(d)_{Re} + 0.516(p)_N$
N(2)–O(2)	0.998 (0.006)	$0.669(sp^{2.03})_N + 0.743(sp^{2.31})_O$	0.998 (0.008)	$0.668(sp^{1.92})_N + 0.744(sp^{2.24})_O$
LP				
N(1)	0.818	$sp^{1.01}$	0.801	$sp^{0.52}$
	0.800	p		
O(1)	0.990	$sp^{0.43}$	0.990	$sp^{0.45}$
	0.934	p	0.743	p
	0.779	p		
N(2)	0.812	$sp^{0.50}$	0.800	$sp^{0.52}$
O(2)	0.990	$sp^{0.43}$	0.990	$sp^{0.45}$
	0.930	p	0.746	p
	0.782	p	0.685	p

BD denotes 2-centre bond; LP denotes lone pair.

The $\sigma_{N(1)–O(1)}$ and $\sigma_{N(2)–O(2)}$ bond orbitals with α- and β-spin are slightly polarized towards the oxygen end, and the s and p nitrogen orbitals and s and p oxygen orbitals take part in N–O bond formation. Five lone pair (LP) NBOs (three with α-spin and two with β-spin) were detected on the O1(1) atom, and six LP orbitals (three with α-spin and three with β-spin) on the O(2) atom. The N(1)–O(1) bond can be treated as a double bond, whereas the N(2)–O(2) bond is a single bond.

In the valence-bond treatment a linear bonding mode of the nitrosyl group may be represented by the resonance forms shown below [11].

A B C D

The results of the NBO analysis indicate that the resonance structure D seems to be the best representation of the bonding in the Re(1)–N(2)–O(2) unit of $[Re(NO)_2Br_2(PPh_3)_2]$, whereas the resonance structure B makes a significant contribution to the Re(1)–N(1)–O(1) moiety.

Supplementary data

Supplementary data for $C_{36}H_{30}Br_{1.91}N_{2.09}O_{2.09}P_2Re$ are available from the CCDC, 12 Union Road, Cambridge CB2 1EZ, UK on request, quoting deposition number 283882.

Acknowledgements

The Gaussian03 calculations were carried out at the Wrocław Centre for Networking and Supercomputing, WCSS, Wrocław, Poland.

References

[1] J.H. Enermark, R.D. Feltham. *Coord. Chem. Rev.*, **13**, 339 (1974).
[2] K.G. Caulton. *Coord. Chem. Rev.*, **14**, 317 (1975).
[3] J.A. McCleverty. *Chem. Rev.*, **79**, 53 (1979).
[4] K.K. Pandey. *Coord. Chem. Rev.*, **51**, 69 (1983).
[5] W.L. Gladfelter. *Adv. Organomet. Chem.*, **24**, 41 (1985).
[6] B.F.G. Johnson, B.L. Haymore, J.R. Dilworth. *Comp. Coord. Chem.*, **2**, 99 (1987).
[7] A.R. Butler, C. Glidewell. *Chem. Soc. Rev.*, **16**, 361 (1987).
[8] G.B. Richter-Addo, P. Legzdins. *Chem. Rev.*, **88**, 991 (1988).
[9] A.R. Butler, C. Glidewell, M.-H. Li. *Adv. Inorg. Chem.*, **32**, 335 (1988).
[10] D.M.P. Mingos, D.J. Sherman. *Adv. Inorg. Chem.*, **34**, 292 (1989).
[11] G.B. Richter-Addo, P. Legzdins. *Metal Nitrosyls*, Oxford University Press, New York (1992).
[12] W.T. Hayton, P. Legzdins, W.B. Sharp. *Chem. Rev.*, **102**, 935 (2002).
[13] J.A. Olabe, L.D. Slep. *Comp. Coord. Chem.*, **1**, 603 (2003).
[14] J.A. McClevetry, M.D. Ward. *Comp. Coord. Chem.*, **2**, 743 (2003).
[15] J.A. McClevetry. *Chem. Rev.*, **104**, 403 (2004).
[16] K.M. Miranda. *Coord. Chem. Rev.*, **249**, 433 (2005).
[17] J.O. Dzięgielewski, K. Filipek, B. Machura. *Polyhedron*, **14**, 555 (1995).
[18] J.O. Dzięgielewski, B. Machura, T.J. Bartczak. *Polyhedron*, **15**, 2813 (1996).
[19] T.J. Bartczak, W. Czurak, J.O. Dzięgielewski, B. Machura. *Polish J. Chem.*, **72**, 633 (1998).
[20] J.O. Dzięgielewski, B. Machura, T. Kupka, T.J. Bartczak, W. Czurak. *Polish J. Chem.*, **72**, 1009 (1998).
[21] J.O. Dzięgielewski, B. Machura, T.J. Bartczak, W. Czurak, J. Kusz, J. Warczewski. *J. Coord. Chem.*, **48**, 125 (1999).
[22] T.J. Bartczak, W. Czurak, J.O. Dzięgielewski, B. Machura, A. Jankowska, J. Kusz, J. Warczewski. *Polyhedron*, **18**, 2313 (1999).
[23] T.J. Bartczak, W. Czurak, J.O. Dzięgielewski, B. Machura, A. Jankowska, J. Kusz, J. Warczewski. *J. Coord. Chem.*, **52**, 361 (2001).
[24] B. Machura, J.O. Dzięgielewski, S. Michalik, T.J. Bartczak, R. Kruszynski, J. Kusz. *Polyhedron*, **21**, 2617 (2002).
[25] M.C. Aragoni, M. Arca, T. Cassano, C. Denotti, F.A. Devillanova, F. Isaia, V. Lippolis, D. Natali, L. Niti, M. Sampietro, R. Tommasi, G. Verani. *Inorg. Chem. Commun.*, **5**, 869.
[26] P. Romaniello, F. Lelj. *Chem. Phys. Lett.*, **372**, 51 (2003).
[27] C.E. Powell, M.P. Cifuentes, A.M. McDonagh, S.K. Hurst, N.T. Lucas, C.D. Delfs, R. Stranger, M.G. Humphrey, S. Houbrechts, I. Asselberghs, A. Persoons, D.C.R. Hockless. *Inorg. Chim. Acta*, **352**, 9 (2003).
[28] J.P. Morral, C.E. Powell, R. Stranger, M.P. Cifuentes, M.G. Humphrey, G.A. Heath. *J. Organomet. Chem.*, **670**, 248 (2003).
[29] STOE & Cie. *X-RED. Version 1.18*. STOE & Cie GmbH, Darmstadt, Germany (1999).
[30] G.M. Sheldrick. *Acta Cryst.*, **A46**, 467 (1990).
[31] G.M. Sheldrick. *SHELXL97. Program for the Solution and Refinement of Crystal Structures*, University of Göttingen, Germany (1997).
[32] G.M. Sheldrick. *SHELXTL: Release 4.1*, Siemens Crystallographic Research Systems, Madison, WI (1990).
[33] M.J. Frisch, G.W. Trucks, H.B. Schlegel, G.E. Scuseria, M.A. Robb, J.R. Cheeseman, J.A. Montgomery Jr, T. Vreven, K.N. Kudin, J.C. Burant, J.M. Millam, S.S. Iyengar, J. Tomasi, V. Barone, B. Mennucci, M. Cossi, G. Scalmani, N. Rega, G.A. Petersson, H. Nakatsuji, M. Hada, M. Ehara, K. Toyota, R. Fukuda, J. Hasegawa, M. Ishida, T. Nakajima, Y. Honda, O. Kitao, H. Nakai, M. Klene, X. Li, J.E. Knox, H.P. Hratchian, J.B. Cross, C. Adamo, J. Jaramillo, R. Gomperts, R.E. Stratmann, O. Yazyev, A.J. Austin, R. Cammi, C. Pomelli, J.W. Ochterski, P.Y. Ayala, K. Morokuma, G.A. Voth, P. Salvador, J.J. Dannenberg, V.G. Zakrzewski, S. Dapprich, A.D. Daniels, M.C. Strain, O. Farkas, D.K. Malick, A.D. Rabuck, K. Raghavachari, J.B. Foresman, J.V. Ortiz, Q. Cui, A.G. Baboul, S. Clifford, J. Cioslowski, B.B. Stefanov, G. Liu, A. Liashenko, P. Piskorz, I. Komaromi, R.L. Martin, D.J. Fox, T. Keith, M.A. Al-Laham, C.Y. Peng, A. Nanayakkara, M. Challacombe, P.M.W. Gill, B. Johnson, W. Chen, M.W. Wong, C. Gonzalez, J.A. Pople. *Gaussian 03*, *Revision B.03*, Gaussian, Inc., Pittsburgh, PA (2003).
[34] A.D. Becke. *J. Chem. Phys.*, **98**, 5648 (1993).
[35] C. Lee, W. Yang, R.G. Parr. *Phys. Rev.*, **B37**, 785 (1988).
[36] P.J. Hay, W.R. Wadt. *J. Chem. Phys.*, **82**, 299 (1985).
[37] E.D. Glendening, A. E. Reed, J. E. Carpenter, F. Weinhold. *NBO*, *Version 3.1*, Theoretical Chemistry Institute, University of Wisconsin, Madison, WI (2001).
[38] A.M. Lebuis, A.L. Beauchamp. *Can. J. Chem.*, **71**, 441 (1993).
[39] D. Bright, J.A. Ibers. *Inorg. Chem.*, **8**, 1078 (1969).

[40] D.H.F. Souza, G. Oliva, A. Teixeira, A.A. Batista. *Polyhedron*, **14**, 1031 (1995).
[41] M. Goldner, B. Geniffke, A. Franken, K.S. Murray, H. Homborg. *Z. anorg. Allg. Chem.*, **627**, 935 (2001).
[42] D. Fenske, N. Mronga, K. Dehnicke. *Z. anorg. Allg. Chem.*, **498**, 131 (1983).
[43] N. Mronga, K. Dehnicke, D. Fenske. *Z. anorg. Allg. Chem.*, **491**, 237 (1982).
[44] N. Mronga, U. Müller, K. Dehnicke. *Z. anorg. Allg. Chem.*, **482**, 95 (1981).
[45] H. Jacobsen, K. Heinze, A. Llamazares, H.W. Schmalle, G. Artus, H. Berke. *J. Chem. Soc., Dalton Trans.*, 1717 (1999).
[46] G.A. Jeffrey, W. Saenger. *Hydrogen Bonding in Biological Structures*, Springer-Verlag, Berlin (1994).
[47] G.R. Desiraju, T. Steiner. *The Weak Hydrogen Bond in Structural Chemistry and Biology*, Oxford University Press, Oxford (1999).
[48] B. Machura, M. Jaworska, R. Kruszynski. *Polyhedron*, **23**, 2523 (2004).
[49] B. Machura. *Polyhedron*, **23**, 2363 (2004).
[50] B. Machura, M. Jaworska, R. Kruszynski. *Polyhedron*, **24**, 267 (2005).
[51] A. Vogler, H. Kunkely. *Coord. Chem. Rev.*, **230**, 243 (2002).
[52] A.E. Reed, L.A. Curtiss, F. Weinhold. *Chem. Rev.*, **88**, 899 (1988).